Comparisons of Total Ion Density Derived from IVM and GNSS TEC on the FORMOSAT-7/COSMIC-2 Mission

Qian Wu[1], Nicholas Michael Pedatella[1], John J. Braun[2], William S. Schreiner[3], Jan Weiss[3], Min-Yang Chou[4], Irina Zakharenkova[5], Iurii Cherniak[5], Douglas Hunt[1], Roderick A. Heelis[6], and Teresa Marie VanHove[1]

[1]National Center for Atmospheric Research (UCAR)
[2]Univ Corp for Atmospheric Res. (UCAR)
[3]University Corporation for Atmospheric Research (UCAR)
[4]Goddard Space Flight Center
[5]COSMIC Program Office, University Corporation for Atmospheric Research
[6]University of Texas at Dallas

November 26, 2022

Abstract

We report on a new method to calibrate the FORMOSAT-7/COSMIC-2 (F7/C2) ion velocity meter (IVM) in-situ ion density data using the Tri GNSS (Global Navigation Satellite System) Radio-occultation System (TGRS) differential total electron content (TEC) data. This calibration is made using collocated measurements from the IVM and TGRS instruments on the same satellite. We found that the IVM ion density is about 8-15% lower than the TGRS derived density at the insertion orbit (~ 710 km) and 5% higher at the mission operation orbit (~ 540 km). Using a linear correction specific to orbit altitude and satellite, an adjustment is implemented for the IVM density data. These corrections remove the offsets between the IVM and TGRS density measurements. We believe the corrected densities eliminate any inter-spacecraft discrepancy in the IVM density data, making it suitable for use in multi-satellite scientific investigations of longitudinal and local time variations and space weather operational applications.

Hosted file

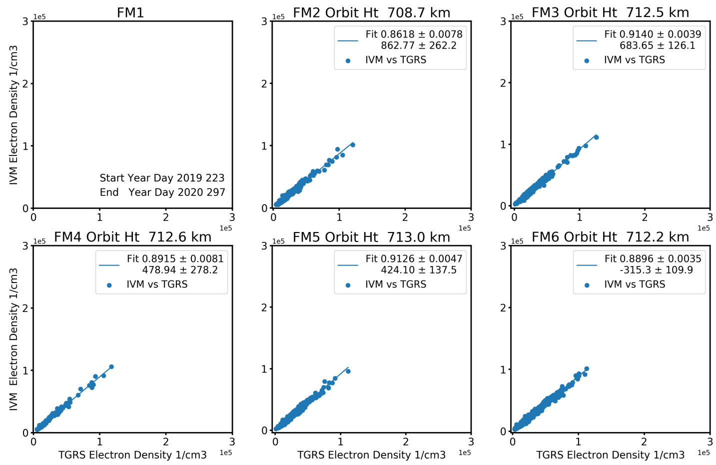
FM1
Start Year Day 2019 223
End Year Day 2020 297
FM2 Orbit Ht 708.7 km
Fit 0.8618 ± 0.0078
862.77 ± 262.2
IVM vs TGRS
FM3 Orbit Ht 712.5 km
Fit 0.9140 ± 0.0039
683.65 ± 126.1
IVM vs TGRS
FM4 Orbit Ht 712.6 km
Fit 0.8915 ± 0.0081
478.94 ± 278.2
IVM vs TGRS
FM5 Orbit Ht 713.0 km
Fit 0.9126 ± 0.0047
424.10 ± 137.5
IVM vs TGRS
FM6 Orbit Ht 712.2 km
Fit 0.8896 ± 0.0035
-315.3 ± 109.9
IVM vs TGRS
IVM Electron Density 1/cm3
TGRS Electron Density 1/cm3

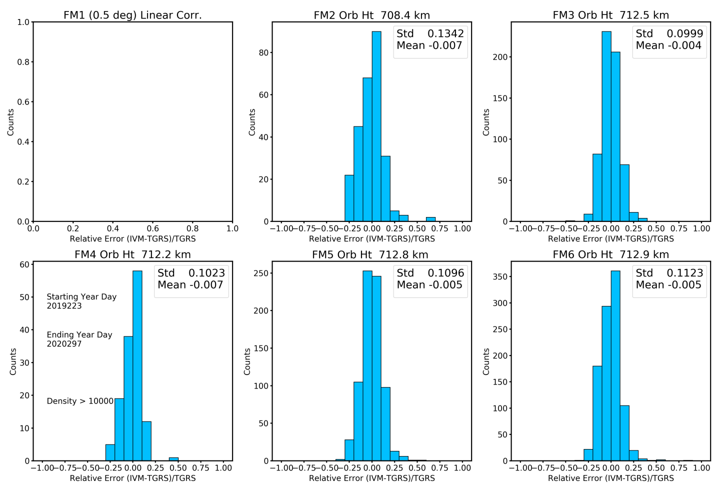
FM1 (0.5 deg) Linear Corr.
FM2 Orb Ht 708.4 km
Std 0.1342
Mean -0.007
FM3 Orb Ht 712.5 km
Std 0.0999
Mean -0.004
FM4 Orb Ht 712.2 km
Std 0.1023
Mean -0.007
Starting Year Day
2019223
Ending Year Day
2020297
Density > 10000
FM5 Orb Ht 712.8 km
Std 0.1096
Mean -0.005
FM6 Orb Ht 712.9 km
Std 0.1123
Mean -0.005
Counts
Relative Error (IVM-TGRS)/TGRS

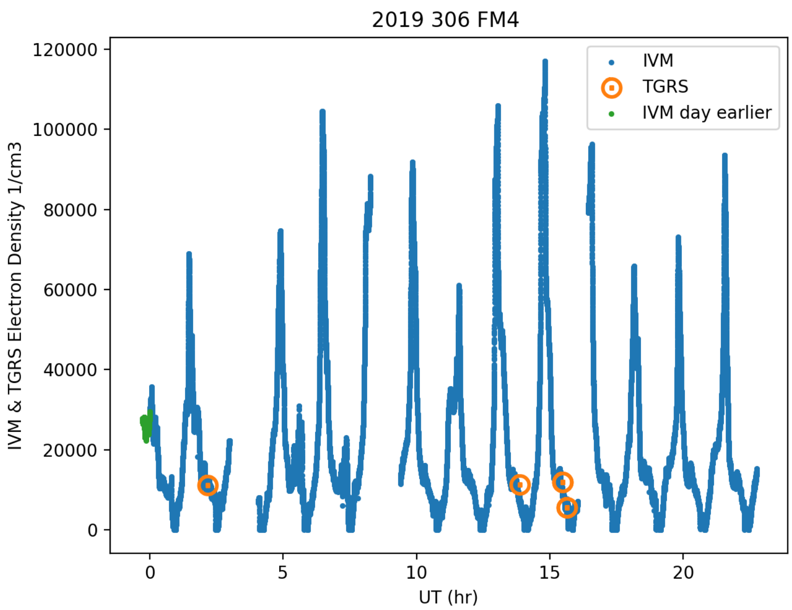
2019 306 FM4
IVM
TGRS
IVM day earlier
IVM & TGRS Electron Density 1/cm3
UT (hr)

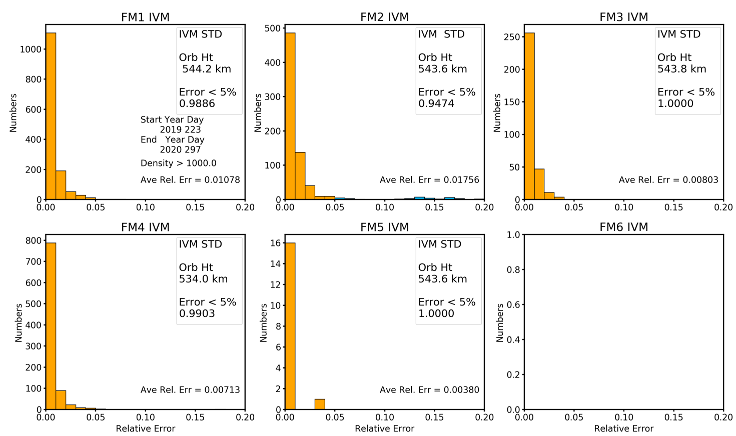
FM1 IVM
IVM STD
Orb Ht
544.2 km
Error < 5%
0.9886
Start Year Day
2019 223
End Year Day
2020 297
Density > 1000.0
Ave Rel. Err = 0.01078
FM2 IVM
IVM STD
Orb Ht
543.6 km
Error < 5%
0.9474
Ave Rel. Err = 0.01756
FM3 IVM
IVM STD
Orb Ht
543.8 km
Error < 5%
1.0000
Ave Rel. Err = 0.00803
FM4 IVM
IVM STD
Orb Ht
534.0 km
Error < 5%
0.9903
Ave Rel. Err = 0.00713
FM5 IVM
IVM STD
Orb Ht
543.6 km
Error < 5%
1.0000
Ave Rel. Err = 0.00380
FM6 IVM
Numbers
Relative Error

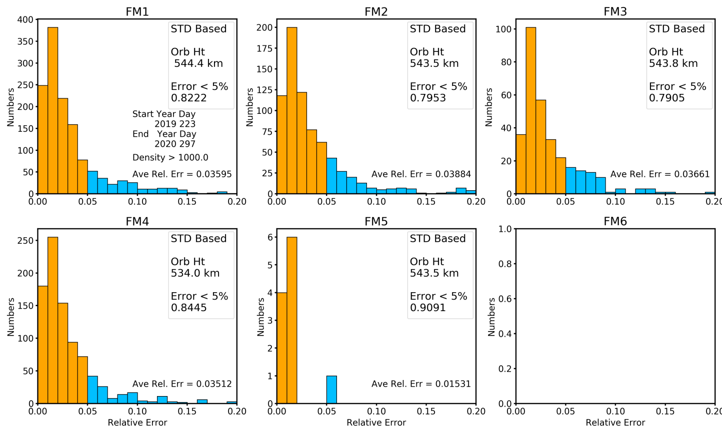
FM1
STD Based
Orb Ht
544.4 km
Error < 5%
0.8222
Start Year Day
2019 223
End Year Day
2020 297
Density > 1000.0
Ave Rel. Err = 0.03595
FM2
STD Based
Orb Ht
543.5 km
Error < 5%
0.7953
Ave Rel. Err = 0.03884
FM3
STD Based
Orb Ht
543.8 km
Error < 5%
0.7905
Ave Rel. Err = 0.03661
FM4
STD Based
Orb Ht
534.0 km
Error < 5%
0.8445
Ave Rel. Err = 0.03512
FM5
STD Based
Orb Ht
543.5 km
Error < 5%
0.9091
Ave Rel. Err = 0.01531
FM6
Numbers
Relative Error

Comparisons of Total Ion Density Derived from IVM and GNSS TEC on the FORMOSAT-7/COSMIC-2 Mission

Qian Wu[1,2], N. M. Pedatella[2,1], John J. Braun[1], W. Schreiner[1], J. Weiss[1], Min-Yang Chou[1], I. Zakharenkova[1], I. Cherniak[1], D. Hunt[1], R. Heelis[3], and T. Vanhove[1]

[1]COSMIC Program/UCP, UCAR, 3090 Center Green Dr., Boulder, Co 80301 USA

[2]HAO/NCAR, 3090 Center Green Dr., Boulder, Co 80301 USA

[3]William B. Hanson Center for Space Sciences, University of Texas at Dallas, Richardson, Texas, USA

Key points:

1. A new method is described to calibrate and validate the FORMOSAT-7/COSMIC-2 IVM ion density data using the differential GNSS slant TEC data.
2. IVM ion density was underestimated (overestimated) at high (low) orbits
3. A linear correction is applied to the IVM ion density, which removed the bias and inter-satellite discrepancies.

Abstract

We report on a new method to calibrate the FORMOSAT-7/COSMIC-2 (F7/C2) ion velocity meter (IVM) in-situ ion density data using the Tri GNSS (Global Navigation Satellite System) Radio-occultation System (TGRS) differential total electron content (TEC) data. This calibration is made using collocated measurements from the IVM and TGRS instruments on the same satellite. We found that the IVM ion density is about 8-15% lower than the TGRS derived density at the insertion orbit (~ 710 km) and 5% higher at the mission operation orbit (~ 540 km). Using a linear correction specific to orbit altitude and satellite, an adjustment is implemented for the IVM density data. These corrections remove the offsets between the IVM and TGRS density measurements. We believe the corrected densities eliminate any inter-spacecraft discrepancy in the IVM density data, making it suitable for use in multi-satellite scientific investigations of longitudinal and local time variations and space weather operational applications.

Introduction

FORMOSAT-7/COSMIC 2 (F7/C2) is a joint Taiwan and United States satellite program that provides neutral atmosphere and space weather data for operational and research purposes [Anthes et al., 2019; Yue et al., 2014]. The primary mission partners are the Taiwan National Space Organization (NSPO), the National Oceanic and Atmospheric Association (NOAA) and the United States Space Force (USSF). The F7/C2 constellation consists of 6 satellites in low-latitude, 24° inclination orbits. The primary payload is the Tri-GNSS

Radio occultation System (TGRS) for atmospheric radio occultation and space weather ionospheric TEC observations [Yue et al., 2014]. All six F7/C2 satellites were initially launched into an insertion orbit of 710 km on June 29, 2019. To obtain uniform sampling across all local times, an orbital precession method was used, where the satellites were lowered sequentially to their operational orbit of 540 km over a period of approximately 18 months. Orbital phasing of the satellites was completed in February 2021. In addition to the TGRS instrument, the Ion Velocity Meter (IVM) instruments on board the F7/C2 measure in-situ ion drifts, temperature, density, and composition [Heelis et al., 2017]. The F7/C2 IVM instrument is nearly identical to that on board the National Aeronautics and Space Administration (NASA) Ionospheric Connections Explorer (ICON) mission [Immel et al., 2017]. The IVM instrument has a long history of making ionospheric measurements [e.g., Hanson et al., 1970]. However, contemporaneous sources of the same parameters are typically only available from ground-based instruments such as incoherent scatter radars (ISR) [e.g., Stoneback et al., 2011]. making it difficult to generate large statistical comparisons.

In-situ measurements of ionospheric density have been compared with GNSS RO observed electron density profiles [Pedatella et al., 2015]. However, the two sets of observations were not always at the same locations and the same time, leading to potential uncertainty due to spatial and temporal inhomogeneities. Nevertheless, a generally good agreement was found between in-situ observations and GNSS RO electron density profiles. Any discrepancies always contain some geophysical variability that arises from spatial and temporal separation, making evaluation of instrument accuracy and precision difficult. Because F7/C2 is an operational mission, there is an urgent need to validate the observations from all instruments to characterize the instrument performance. One important advantage of F7/C2 is that it includes both GNSS RO and in-situ ionospheric instruments. Similarly, the CHAMP mission also carried both GNSS RO and an in-situ Planar Langmuir Probe (PLP) [Jakowski et al., 2002]. Yue et al. [2011] have used GNSS slant TEC data to derive the on-orbit electron density and compared it with the PLP in-situ density based on the method of Syndergaard [2004]. This method uses slant TEC to derive the on-orbit electron density based on the motion of the LEO satellite relative to the GNSS satellite. When the LEO orbital motion direction is nearly parallel to the direction of the GNSS satellite, the changes in the slant TEC can be used to calculate the density by dividing the change in the TEC by the change in distance between the GNSS and LEO satellites. While the comparisons showed mostly good agreement, there was also a large spread of data. Overall, the ionospheric density derived from GNSS RO slant TEC observations was found to be ~10% larger than the PLP in-situ observation, which Yue et al. [2011] attributed to variations between the satellite velocity vector and the line-of-sight to the GNSS-satellite in the RO observation. The RO observations have contributions from the ionosphere below the orbital height, which usually is higher than that on orbit. Syndergaard [2004] used distance variations up to 372 km, which can cause the tangent height to be ~ 9 km lower than the orbital height. Because of the large discrepancy, it was not possible to characterize any possible bias in the PLP observation.

In this study, we use a similar method as Yue et al. [2011] and Syndergaard [2004] applied to derive the in-situ ionospheric density from the GNSS receivers. An important aspect of this method is the selection of the distance traveled by the LEO. Shorter distance traveled will minimize geometric errors, but can lead to large errors due to small differences in slant TEC. Longer distance traveled makes slant TEC variation larger and relative error smaller, though the geometric error will be larger due to sampling more ionosphere below the orbit. Hence, a balance is needed. One thing we do not need to worry about is spatial-temporal coincidence since the IVM and GNSS RO derived density are at nearly the same location and time. Hence, we can set a more stringent criterion in data selection, which entails a short traveling distance for the LEO satellite. We will show that we have found a viable method to derive the total plasma density from the GNSS-RO observations that is sufficiently robust to provide a statistical comparison with the total density derived from the IVM. One of the most significant aspects of F7/C2 is the availability of the six individual IVMs on six satellites providing simultaneous observations across a range of local times and longitudes. This enables multi-satellite investigations of, for example, variations associated with nonmigrating tides and planetary waves.

The paper is organized as follows, we first describe our methodology and present comparison results for the F7/C2 satellites at insertion (~710 km) and mission (~540 km) orbits. We then establish quantitative relationships between the various data sources. Last, we discuss our findings and summarize our results.

Differential TGRS Slant TEC Derived Density

The F7/C2 GNSS receiver is a NASA Jet Propulsion Laboratory (JPL) designed TGRS (Tien et al., 2012), which currently observes signals from the GPS and GLONASS constellations. The ability to observe Galileo signals can potentially be added in the future. By calculating the phase differences between the L1 and L2 signals, the relative slant TEC can be derived due to the frequency dependence of the signal propagation through the ionosphere. The slant TEC data are usually inverted to profiles of electron density for space weather applications. Under certain conditions, the slant TEC can be used to derive the electron density without using an inversion method, which requires the assumption of horizontal homogeneity. When an F7/C2 satellite travels in the direction parallel or anti-parallel to the line-of-sight to a GNSS satellite, the change in the distance between the F7/C2 and GNSS satellites leads to a change in slant TEC. By taking the derivative of the slant TEC with respect to distance, we can derive the in-situ electron density values, which can be assumed to be equal to the ion densities under charge neutrality. By not using an inversion, this method yields electron densities that are more accurate, when the line-of-sight conditions are met. Figure 1 shows the geometry of how slant TEC observations are used to derive the in-situ electron density by identifying instances when the F7/C2 satellite velocity vector is parallel or anti-parallel with the line-of-sight to the GNSS satellite that is being observed. The F7/C2 has two POD (Precise Orbit Determination) antennae (#1 in the aft direction and #2 in the fore direction). Both can be used to derive the electron density.

The necessary geometry between a GNSS transmitter satellite and a F7/C2 satellite only occurs a few times per day. We have to set a criterion for selecting when the geometry is considered sufficient to calculate the electron density from the slant TEC observations. After trying with 1.0°, 0.75°, 0.5°, and 0.25° cone angles (i.e., the angle between the F7/C2 velocity vector and the GNSS transmitter satellite), we found that 0.5° is the smallest cone angle that will give us 9 pairs of data points within it. The 0.25° cone angle is too small to have 9 pairs of data points. From 2019 day 229 to 2020 day 298, the number of TGRS passes that can be used for different cone angles are 25830 (1.0°), 18087 (0.75°), 9542 (0.5°), and 0 (0.25°). Because we need to perform a multi-sample average to reduce the random error of the derived in-situ electron density, 0.5° cone angle was selected. Additionally, though a larger cone angle would provide a greater number of points for comparison, it would increase geometrical errors. For each satellite, the 0.5° cone angle will have roughly five passes either in front of or behind the satellite travel direction in one day. Figure 2 shows the TGRS slant TEC derived electron density compared to the IVM ion density for one day. The results in Figure 2 show a good agreement between the TGRS slant TEC in-situ electron density and IVM ion density, demonstrating the utility of this method.

While five comparisons per day is not a high number, it is significantly more frequent than could be obtained by other methods, such as comparison with ground-based or other satellite observations. In selecting the distance traveled by the F7/C2 satellite, we settled on 2-second separation between the two TEC samples, which is about 15 km in distance based on the F7/C2 satellite orbital speed. The sample rate for both the IVM density and TGRS slant TEC is one second. The path length traveled by the satellites is determined using TGRS orbit solutions, which have accuracy better than 10 centimeters. In comparison to the distance traveled (~15 km), the error due to orbit accuracy is very small and can be ignored.

The geometry of the measurement has some similarities to the Gravity Recovery and Climate Experiment (GRACE) twin satellite observation of electron density based on the dual frequency beacon signals from one satellite to another [Lee et al., 2011; Xiong et al., 2010]. In the case of GRACE, the distance between the two satellites is about 200 km. In our case, the distance is ~ 15 km traveled by the F7/C2 satellite. Unfortunately, GRACE was not carrying any in-situ ion density instrument for direct simultaneous comparison.

Precision of the Differential TGRS TEC Derived Density

The error in the TEC measurements is determined by the GNSS phase error which is inversely proportional to the GNSS signal to noise ratio (SNR). Based on the SNR values we can estimate the GNSS phase error for both the L1 and L2 signals. SNR values are included in the F7/C2 podTc2 data files along with the

TEC values. In the following, we estimate the percentage error for the TGRS derived electron density. Though we derived the electron density from both the GPS and GLONASS signals, for consistency, in this study we only present results based on the GPS observations. The in-situ electron density is derived as:

$$\mathrm{Density}_{\mathrm{electron}} = \frac{\mathrm{dTEC}}{\mathrm{ds}} \qquad (1),$$

where *dTEC* is the TEC difference between the two samples that are 2-seconds apart, and *ds* is the distance the F7/C2 satellite traveled in 2 seconds.

The percentage error for the electron density is expressed as follows:

$$\delta\mathrm{Density}^2_{\mathrm{electron}}/\mathrm{Density}^2_{\mathrm{electron}} = \left(\frac{\mathrm{dTEC}}{\mathrm{dTEC}}\right)^2 + \left(\frac{\mathrm{ds}}{\mathrm{ds}}\right)^2 \qquad (2).$$

The uncertainty in distance measurements (*ds*) for the F7/C2 is about 10 cm, while *ds* ~ 1.5x10^6 cm. Hence, the second term in Eqn. 2 is very small and can be ignored. Therefore, the percentage error is mainly determined from the first term in Eqn. 2.

The error in the TEC is related to the GNSS phase error, which equals 1 rad / SNR. Because TEC is derived based on L1 and L2 signal phase, we have:

$$(\delta dTEC)^2 = (\delta L_1\mathrm{phase})^2 + (\delta L_2\mathrm{phase})^2 \qquad (3),$$

where, δL_1phase, δL_2phase are the L1 and L2 phase error in TECU, which are listed in Table 1. The coefficients of ~2.85 converts GPS phase error in 1 ns to TECU, the factor 300 comes from the speed of light to convert from mm to ns in the formula [e.g., Mylnikova et al., 2015]. The formula for GLONASS is like GPS with a ns to TECU factor of ~2.9. To convert to density in 1/cm3 from TECU (10^{12} e/cm^2), we divide the values with 15 km distance (1.5x10^6cm). Table 1 lists precision for individual L1 and L2 band contributions. The overall (combined L1 and L2) absolute density precision for typical SNR values of GPS are 1270 cm-3 (L1 with L2P), 693 cm-3 (L1 with L2C), and 703 cm-3 for GLONASS.

Table 1. GPS and GLONASS Signal Phase Errors

GNSS Signals	Phase Error (mm)	Phase Error (TECU)	Typical SNR	Density (1/cm3)
GPS L1 (1 rad/SNR)	/(2 SNR)	(2.85/3.)/(2 SNR)		
GPS L2 (1 rad/SNR)	/(2 SNR)	(2.85/3.)/(2 SNR)	L2P 200, L2C 400	615
GLONASS L1 (1 rad/SNR)	/(2 SNR)	(2.9/3.)/(2 SNR)		
GLONASS L2 (1 rad/SNR)	/(2 SNR)	(2.9/3)/(2 SNR)		

Within the 0.5° cone, we select 9 pairs of TEC samples (2-seconds apart) to derive 9 density values, which are then averaged to obtain a single electron density. That increases the density precision by a factor of 3. We have typical absolute density precisions for 9-pair averages of 423 cm-3 (GPS L2P), 231 cm-3 (GPS L2C), and 234 cm-3 for GLONASS. We also estimate the percentage precision of the derived density by using the SNRs of the L1 and L2 signals. Figure 3 shows the distribution of the percentage precision of TGRS derived electron density using the formula in Table 1 (SNR based) for the lower orbit F7/C2 (high orbit results are similar and not shown). We do not use data with electron density smaller than $10^3/\text{cm}^3$, which is the lower limit for the IVM density measurement [*Heelis et al.*, 2017]. FM5 was just transferred to the lower orbit and FM6 was still at high orbit for the time period considered. Consequently, we have only a few data points from FM5 and none from FM6. We also estimate the standard deviation of the 9 density samples to gauge observational precision, which combines the instrument precision and geophysical variation (Figure 4).

IVM (Ion Velocity Meter)

The IVM instrument measures the ion density, temperature, composition, and drift. The F7/C2 IVM Level 2 (ivmLv2) files were used. The temporal resolution of the observations is 1 second. The instrument operates identically to that on the ICON mission [Heelis et al. [2017]. The total ion density is derived from the Retarding Potential Analyzer, that presents a planar aperture that views along the spacecraft velocity vector. Behind the aperture are a series of planar grids that precede a solid collector at which the ion current, proportional to the flux of incident ions, is measured. For measurement of the total ion density, all grids are grounded with the exception of a negatively biased suppressor grid that prevents access to the collector by thermal electrons. Since the sensor is moving supersonically with respect to the ions, the total ion density N_i is derived from the ion current I_s by the expression $N_i = \frac{I_s}{qA_{\text{eff}}V_r}$, where q is the electron charge, A_{eff} is the effective collection area behind the aperture and V_r is the velocity of the plasma along the look direction of the sensor. The effective collection area of the sensor is determined by the aperture physical dimensions and from the optical transparency of the grids, determined by the wire size and wire spacing. Uncertainty in the ion density from this source is ~2%. The current itself is determined from the output of a linear ranging electrometer, that is calibrated in the laboratory before flight, to verify an uncertainty in the current of 1% or $5\text{x}10^{-11}$ A. The ram velocity is dominated by the spacecraft orbital speed, which is known to very high precision. However, this velocity also includes the ambient ion drift along the look direction of the sensor, that is derived from the RPA and may vary by ±200 m/s. Utilizing this variation itself we may derive a maximum uncertainty in the ion density of ±200/7500 ~±3% from this source. Combining these know uncertainties we may expect the total ion density to be derived with an uncertainty of <4% if the electrostatic environment of the spacecraft does not change the ambient ion distribution around the sensor or the ion collection properties of the sensor.

IVM and TGRS Density Comparison

We separate the data for high and low orbits, because the geophysical environment (ion composition, density, temperature, and drift) surrounding the spacecraft is different. As mentioned previously, the F7/C2 satellites were sequentially transferred to lower orbits to allow orbital precession to separate the satellites equally in local time. The last F7/C2 satellite (FM6) completed its transfer in early 2021. Hence, in our analysis, we exclude some FMs in either high or low orbits. The low orbit data for FM5 and FM6 are mostly absent. FM1 doesn't have high orbit data, as it was transferred to the lower orbit soon after launch. Scatter plots comparing the IVM ion density and TGRS TEC derived electron density for each FM at high and low altitudes are shown in Figures 5 and 6, respectively. The data cover the time period from 2019 day 223 to 2020 day 297. To reduce representative sampling errors, we averaged the IVM data across 9 samples to match the TGRS sample volume. Linear least squares fittings were performed to derive a linear relationship between the two observations. Figure 5 shows that the IVM density values are 8 to 15 percent smaller than their TGRS counterparts for data collected when the satellites were at their insertion orbit of 710 km. For data collected at the mission orbit altitude of 540 km the IVM densities are about 5 percent higher than those derived from the TGRS (Figure 6). Tables 2 and 3 provide the slope and intercept along with the R-values that relate the total ion densities derived from the IVM and the TGRS. Based on the least squares fitting coefficients (TGRS vs IVM) we calculated the correction coefficients for the IVM density, which are provided in Tables 2 and 3 for the high and low orbits, respectively. Note that the low orbit coefficients for FM5 and FM6 are the average results of FM1 to FM4.

Table 2. Linear coefficients, *A* and offsets, *B* relating IVM and TGRS derived plasma density as $N_{TGRS}= AN_{IVM}+B$ and correlation coefficients for high latitude orbits

FM	1	2	3	4	5	6
A	No data	1.1553	1.0943	1.1335	1.0783	1.1164
B	No data	292.82	798.15	278.04	1140.0	1667.4
Corr Coeff R	No data	0.99	0.99	0.99	0.99	0.99

Table 3 Linear coefficients, *A* and offsets, *B* relating IVM and TGRS derived plasma density as $N_{TGRS}= AN_{IVM}+B$ and correlation coefficients for low altitude orbits

FM	1	2	3	4	5	6
A	0.9422	0.9645	0.9639	0.9632	0.9642	0.9642
B	-7448.	-3423.	-2555.	-3492.	-2989.	-2989.
Corr Coeff R	0.99	0.99	0.99	1.00	No data	No data

Discussion

It is uncommon to have two measures of ionospheric density from the same satellite. A similar configuration of sensors was available on the Swarm satellite but in this case the POD antennas limit the ability to sample along the path of satellite motion due to limits in how low the signal is tracked (elevation limit at 20 deg). However, the F7/C2 TGRS instrument allows frequent opportunities to view approximately parallel or antiparallel to the satellite velocity vector and thus provides a unique opportunity to compare measurements of the total ion density from two sources. This allows both data sets to be normalized to each other allowing them to be used together to produce a larger more spatially distributed data set. While the TGRS derived density self-determined precisions are small (based on the standard deviation), the inter-instrument (IVM-TGRS) discrepancy is larger indicating there are still uncaptured variations in the observations of either instrumental or geophysical origin. Nevertheless, first order linear relationships between the two data sets can be established that account for systematic but unspecified uncertainties in observational configurations associated with each data set taken at high and low altitudes.

We note that the IVM derived total density in high orbits is smaller than the TGRS derived values whereas in the lower orbits, the IVM derived density data are slightly larger than the TGRS densities.

In the early comparison between the in-situ PLP and GNSS TEC derived ion density from the CHAMP satellite, Yue et al. [2011] found PLP values about 10% smaller than the GNSS TEC derived data and attributed the bias to the geometrical factor of the GNSS observation. The geometrical issue arises from the GNSS TEC sampling method, which uses least squares fitting with ionospheric observations at lower altitudes. In our analysis, we minimize ionospheric observations below the satellite orbit by using the smallest possible cone angle and time separation between samples. We have two opposite biases with the IVM density at high and low orbits, which suggests that our method does not have the same geometric factor induced bias as in the Yue et al. [2011] case. Moreover, the difference in sign between IVM and TGRS derived ion densities, is dependent on the altitude of observation and thus the distance from the O+/H+ transition height. This suggests that discrepancies between the two measurements may be more related to the ionospheric composition and the environment of the topside ionosphere. Most significant in this regard might be the effective collection area of the IVM and its dependence on the plasma composition and temperature. The presence of a conducting ground plane around the sensor minimizes these effects by minimizing changes transverse to the sensor look direction. However, further investigations into variations dependent on season, local time and latitude may reveal other systematic conditions that produce these differences that are of order 10%

After aligning the IVM and TGRS derived ion density we find that the standard deviations of the differences remain significant ranging from 16 percent to 9 percent as shown in Figures 7 and 8 for high and low orbit respectively.

This deviation is significantly larger than the previously derived precision of the TGRS derived density of 3 percent (figure 4) or the deviation among the assembled samples that make up the 9 second interval of IVM data used for comparison, which is less than 2% (Figure 9). This also suggests that the dynamics of the topside environment deserves further consideration as a source of variability between the measurement techniques.

Nevertheless, the linear correction has achieved its goal of removing the offset in the IVM density data from both high and low orbits. We also removed any inter-spacecraft discrepancy readying the data for cross-satellite analysis to study nonmigrating tides and other longitudinal nonuniformities in the ionosphere. GNSS RO observations are becoming more common in space missions large and small. This method can help validate other ionospheric instruments on-board future satellites. It can help remove inter-satellite and inter-mission discrepancy in in-situ ion density observations. Thus, we have more incentive to include a GNSS receiver as part of future space missions for calibrating in-situ ion density.

Summary

We summarize our key findings as follows:

1. We used a new differential TEC method to validate the F7/C2 IVM ion density data.
2. We found that at high orbit (~710 km) the IVM densities were about 8 to 15 percent lower than the TGRS derived density, whereas at lower orbits (~540 km) they were about 5 percent higher.
3. A linear correction was applied to the IVM density, which removes the offset. We verify that the corrected IVM densities are fully consistent with the TGRS derived density afterward.
4. More importantly, we also removed inter-satellite discrepancy in the IVM density, which is ready for scientific and space weather applications.

Acknowledgement:

This work was supported by Air Force Contract FA8803-19-C-0004. National Center for Atmospheric Research is supported by the National Science Foundation corporative agreement 1852977 and grants AGS-2054356 AGS-2120511 and NASA grants 80NSSC20K0199, NNX17AG69G, 20-GIGI20-007. The TGRS Level 1 podTc2 data and IVM level 2 ivmLv2 data can be found on the UCAR COSMIC Data Analysis and Archive Center (http://cdaac-www.cosmic.ucar.edu).

References:

Anthes, R. A., & Schreiner, W. S. (2019). Six new satellites watch the atmosphere over Earth's equator. Eos (Washington. DC), doi: 10.1029/2019EO131779

Hanson, W. B., S. Sanatani, D. Zuccaro, T. W. Flowerday (1970), Plasma measurements with the retarding potential analyzer on Ogo 6, J. Geophys. Res., 75, 5481-5501, https://doi.org/10.1029/JA075i028p05483.

Heelis, R.A., Stoneback, R.A., Perdue, M.D. *et al.* (2017), Ion Velocity Measurements for the Ionospheric Connections Explorer. *Space Sci Rev* **212,** 615–629 (2017). https://doi.org/10.1007/s11214-017-0383-3

Jakowski, N., A. Wehrenpfennig, S. Heise, C. Reigber, H. Lühr, L. Grunwaldt, and T. K. Meehan (2002), GPS radio occultation measurements of the ionosphere from CHAMP: Early results, Geophys. Res. Lett., 29(10), 1457, doi:10.1029/2001GL014364.

Immel, T.J., England, S.L., Mende, S.B. *et al.* (2018), The Ionospheric Connection Explorer Mission: Mission Goals and Design. *Space Sci Rev* **214,** 13. https://doi.org/10.1007/s11214-017-0449-2.

Lee, CK., Han, SC., Bilitza, D. *et al.* Validation of international reference ionosphere models using in situ measurements from GRACE K-band ranging system and CHAMP planar Langmuir probe. *J Geod* **85,** 921–929 (2011). https://doi.org/10.1007/s00190-011-0442-6.

Mylnikova, A. A., Yu. V. Yasyukevich, V.E. Kunitsyn, A. M. Padokhin (2015), Variability of GPS/GLONASS differential code biases, Results in Physics, 5, 9-10, http://dx.doi.org/10.1016/j.rinp.2014.11.002.

Pedatella, N. M., Yue, X., and Schreiner, W. S. (2015), Comparison between GPS radio occultation electron densities and in situ satellite observations, *Radio Sci.*, 50, 518– 525. doi:10.1002/2015RS005677.

Stoneback, R. A., Heelis, R. A., Burrell, A. G., Coley, W. R., Fejer, B. G., and Pacheco, E. (2011), Observations of quiet time vertical ion drift in the equatorial ionosphere during the solar minimum period of 2009, *J. Geophys. Res.*, 116, A12327, doi:10.1029/2011JA016712.

Syndergaard, S., D. C. Hunt, W. S. Schreiner, and C. Rocken (2004), In situ electron density in low earth orbit from radio occultation data, Abstract SF52A-08 presented at 2004 Fall Meeting, AGU, San Francisco, Calif., 13–17 Dec.

Tien, J. Y., Okihiro, B. B., Esterhuizen, S. X., Franklin, G. W., Meehan, T. K., Munson, T. N., . . . Young, L. E. (2012). Next Generation Scalable Spaceborne GNSS Science Receiver. In Proc. 2012 int. tech. meet. inst. navig. (pp. 882–914). Newport Beach, CA.

Xiong, C., Park, J., Lühr, H., Stolle, C., and Ma, S. Y.: Comparing plasma bubble occurrence rates at CHAMP and GRACE altitudes during high and low solar activity, Ann. Geophys., 28, 1647–1658, https://doi.org/10.5194/angeo-28-1647-2010, 2010.

Yue, X., W. S. Schreiner, C. Rocken, and Y.-H. Kuo (2011), Evaluation of the orbit altitude electron density estimation and its effect on the Abel inversion from radio occultation measurements, Radio Sci., 46, RS1013, doi:10.1029/2010RS004514.

Yue, X., Schreiner, W. S., Pedatella, N., Anthes, R. A., Mannucci, A. J., Straus, P. R., & Liu, J.-Y. (2014). Space Weather Observations by GNSS Radio Occultation: From FORMOSAT-3/COSMIC to FORMOSAT-7/COSMIC-2. Sp. Weather, 12(11), 616–621. doi: 10.1002/2014SW001133.

Figure captions

Figure 1. Geometry for differential TGRS slant TEC measurements used to derive in-situ electron density. Any GNSS transmitter that passes within 0.5° of the velocity (or anti-velocity) direction of the LEO satellite can be used to derive the in-situ electron density. The in-situ electron density is derived from either the fore or aft POD antenna, depending on the location of the GNSS transmitter. The distance traveled by the LEO is exaggerated to illustrate the method.

Figure 2. 2019 Day 306 FM4 IVM (blue dots) and TGRS derived density (orange circles) comparison. Good agreement between the two measurements is apparent. IVM data from the previous day is shown in green. The IVM density has one second temporal resolution.

Figure 3. The precision of the TGRS derived density based on the SNR values of the GPS L1 and L2 signals using the formula in Table 1. Because we used a 9-sample average the precision is divided by a factor of 3 (square root of 9). The orange color marks the bins with relative error less than 5%, which is the requirement for the IVM density. More than 90 percent of the time the precision is better than 5%. Data from FM6 is omitted in this comparison as it had not been lowered to its mission altitude of 540 km.

Figure 4. The plot is in the same format as Figure 3 but for the TGRS derived electron density precision based on the 9-sample standard deviation. Because the density is the average of the 9 samples, the precision equals the 9-sample standard deviation divided by square root of 9 (3). The averaged precision is 3% for FM1 to FM4, which is better than 5%. FM5 and 6 do not have enough data at the mission altitude of 540 km to be used in the analysis.

Figure 5. IVM vs TGRS density comparison for high orbit. FM1 does not have high orbit data. The linear fit lines are also plotted and fitting coefficients are given in the legends. The fitting slope shows the IVM densities are 8 to 15 percent smaller than the TGRS measurements. The plot scales are in 1.e5 /cm3.

Figure 6. Same as Figure 5 but for low orbit. FM5 and 6 have very few or no data points in the time period used for the analysis. The fitting slopes show the IVM densities are about 4 to 6 percent higher than the TGRS values, which is opposite to the high orbit case.

Figure 7. IVM vs TGRS relative discrepancy distribution after the linear cor-

rection to the IVM density. FM1 has no high orbit data. The density values less 1e4 /cm3 are not included in this statistic. The mean discrepancy is mostly less than 1 percent. The standard deviation ranges from 10 to 13 percent.

Figure 8. Same as Figure 7 but for low orbit. The standard deviation of the distribution ranges from 9 to 16 percent. FM5 data numbers are too low to be significant. FM6 does not have low orbit data for the period used for analysis.

Figure 9. Precision of the IVM density based on the standard deviations of the 9 samples used to calculate the averaged value. The precision of the IVM densities is less than 1.7 %.